International Biodeterioration & Biodegradation 133 (2018) 230–237

Contents lists available at ScienceDirect

International Biodeterioration & Biodegradation

journal homepage: www.elsevier.com/locate/ibiod

Acetylation increases relative humidity threshold for ion transport in wood cell walls – A means to understanding decay resistance

Christopher G. Hunt[a], Samuel L. Zelinka[a], Charles R. Frihart[a], Linda Lorenz[a], Daniel Yelle[a], Sophie-Charlotte Gleber[b,c], Stefan Vogt[b], Joseph E. Jakes[a,*]

[a] USDA Forest Service, Forest Products Laboratory, Madison, WI, USA
[b] Argonne National Laboratory, Advanced Photon Source, Lemont, IL, USA
[c] Institute for X-ray Physics, Georg-August Universität, Göttingen, Germany

ARTICLE INFO

Keywords:
Decay resistance
Diffusion
X-ray fluorescence
Humidity
Acetylated wood
Reduced equilibrium moisture content
Wood modification

ABSTRACT

The improved fungal decay resistance exhibited by modified wood has been attributed to inhibited diffusion of decay precursors and subsequent degradation products through the wood cell wall. However, data relating the effect of modification to diffusion through wood cell walls is lacking. Synchrotron X-ray fluorescence microscopy paired with an *in situ* humidity chamber was used to observe the transport of an implanted model metabolite, potassium (K^+) ions, in wood cell walls as a function of relative humidity (RH) and extent of the wood modification acetylation. The RH threshold for K^+ transport in wood cell walls increased with increasing levels of acetylation between 0 and 20 wt percentage gain (WPG), which clearly indicates that acetylation inhibits ion transport in the modified wood cell walls. The reduced equilibrium moisture content (EMC_R or moisture based on wood polymer mass) thresholds were also calculated, but the trend of EMC_R thresholds with WPG was inconclusive. Although the results provided support to the proposed mechanism that diffusion inhibition in acetylated wood caused decay resistance, the results could not confirm that diffusion inhibition was the most important mechanism. The observed inhibition of K^+ transport in acetylated wood should motivate additional work to understand how chemical modifications affect cell wall diffusion and the implications for producing decay-resistant wood.

1. Introduction

Wood is a desirable building material because it is economical, it is renewable, it typically requires relatively little energy to produce, and it sequesters carbon (Bergman et al., 2014; Jakes et al., 2016). One of the limitations of wood is that it is subject to decay when exposed to high moisture conditions. Wood decay is primarily caused by filamentous fungi, which are characterized as either brown, white, or soft rot fungi. Brown rot fungi pose an increased threat to wood and wood-based materials due to their prevalence on coniferous species, which predominate the construction market, and because they rapidly depolymerize all wood polymers, which can lead to rapid structural failure (Curling et al., 2002; Martinez et al., 2005; Arantes and Goodell, 2014) These fungi have 1–3 μm diameter hyphae that can grow through the open micron-scale spaces in the wood cellular structure and adhere to interior surfaces. In the initial stages of brown rot, these fungi secrete low-molecular-weight reactants or oxidant precursors that diffuse into the wood cell wall to oxidize and cleave cell wall polymers (Hammel et al., 2002; Arantes and Goodell, 2014). In brown rot, the oxidative mechanism is thought to be dominated by the fenton reaction of Fe^{2+} with hydrogen peroxide (H_2O_2) to create the highly reactive hydroxyl radical (Suzuki et al., 2006; Arantes and Goodell, 2014). Therefore H_2O_2 and Fe^{2+} inside the cell wall must be continually replenished by enzymatic action in the lumen. Fungal enzymes make H_2O_2 directly but are thought to reduce Fe via small diffusible reducing agents (Kerem et al., 1998; Tanaka et al., 1999; Cohen et al., 2002; Arantes and Goodell, 2014). White rot fungi are thought to produce a variety of diffusible oxidants including, but not limited to, veratryl alcohol cation radical, fatty acid peroxyl radicals, and manganese III chelates (Harvey et al., 1986; Popp et al., 1990; Tanaka et al., 1999). All these oxidants,

Abbreviations: WPG, Weight Percentage Gain; RH, Relative Humidity; EMC, Equilibrium Moisture Content; EMC_R, Reduced Equilibrium Moisture Content; XFM, X-ray Fluorescence Microscopy; ROI, Region of Interest; AMU, Atomic Mass Unit

* Corresponding author. Research Materials Engineer, USDA Forest Service, Forest Products Laboratory, One Gifford Pinchot Drive, Madison, WI, 53726, USA.
E-mail addresses: cghunt@fs.fed.us (C.G. Hunt), szelinka@fs.fed.us (S.L. Zelinka), cfrhart@fs.fed.us (C.R. Frihart), llorenz@fs.fed.us (L. Lorenz), dyelle@fs.fed.us (D. Yelle), sophie-charlotte.august@phys.uni-goettingen.de (S.-C. Gleber), svogt@anl.gov (S. Vogt), jjakes@fs.fed.us (J.E. Jakes).

https://doi.org/10.1016/j.ibiod.2018.06.014
Received 22 February 2018; Received in revised form 31 May 2018; Accepted 16 June 2018
0964-8305/ Published by Elsevier Ltd.

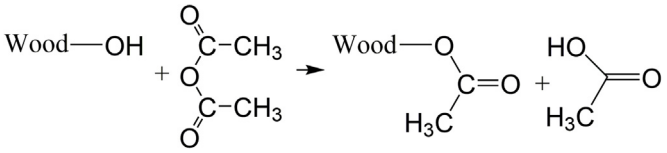

Fig. 1. Acetylation reaction.

after diffusing into and attacking the cell wall, release soluble sugars that then diffuse out of the cell wall and can be taken up as an energy source by the fungus (ten Have and Teunissen, 2001; Martinez et al., 2005; Arantes and Goodell, 2014). To protect wood from decay, copper-based preservative treatments are often prescribed. However, these wood preservatives are registered pesticides and their availability depends on future regulations and maintaining their registration with environmental regulators (Lebow, 2004). Nontoxic alternatives to wood preservatives are being sought as manufacturers and consumers are increasingly demanding decay-resistant wood products with non-biocidal treatments (Hill, 2011; Mantanis, 2017; Sandberg et al., 2017).

An alternative to preservative treatments is to make wood resistant to decay by modifying wood chemistry. Although numerous wood modification methods have been developed and found effective, acetylation is currently the most widely studied and is finding commercial success (Hill, 2006; Mantanis, 2017). During acetylation, wood is treated with acetic anhydride and the hydroxyl groups on wood polymers are replaced with acetate esters (Fig. 1). The effectiveness of the treatment depends on the extent of modification, which can be quantified using weight percentage gain (WPG), defined as the change in mass resulting from the modification divided by the original wood mass. Mass increases because the acetate ester (59 AMU) is heavier than the hydroxyl group (17 AMU) it replaces. Volumetric swelling of the wood cell wall is approximately the same as WPG (for example, 12% dry volume swelling at 12 WPG) (Hill and Graham, 2004). This irreversible swelling from acetylation decreases pore volume and the amount of water vapor that is sorbed at a given relative humidity (RH) (Stamm and Tarkow, 1947; Hill, 2006; Engelund et al., 2013; Popescu et al., 2014). With regards to decay resistance, acetylation to 20 WPG is very effective at inhibiting decay, whereas 10 WPG is only mildly inhibitory to decay (Stamm and Baechler, 1960; Ibach and Rowell, 2000; Larsson Brelid et al., 2000; Hill 2006, 2009).

Despite the empirically known effectiveness of acetylation, the material property changes caused by acetylation that lead to the improved decay resistance are not thoroughly understood and continue to be an active topic of research (Rowell et al., 2009; Ringman et al., 2014; Alfredsen et al., 2015; Hosseinpourpia and Mai, 2016b; Thybring, 2017). Proposed mechanisms for how wood modifications, including acetylation, inhibit decay, along with supporting references and analyses of which mechanisms are most likely to contribute, are available elsewhere (Ringman et al., 2014; Zelinka et al., 2016). The proposed mechanisms for decay resistance of modified wood include (1) acetylated hemicelluloses do not serve as a nutrient source for fungi (Rowell et al., 2009; Rowell, 2015); (2) fungal degradative enzymes that break down modified wood polymers are inhibited (Rowell, 2005; Rowell et al., 2009); (3) fungal degradative enzymes are unable to enter cell wall because micropores are blocked by the modification (Hill et al., 2005); and (4) diffusion within the cell wall is inhibited because the modification decreases the wood equilibrium moisture content (EMC) (Papadopoulos and Hill, 2002; Boonstra et al., 2007; Jakes et al., 2013; Xie et al., 2015; Hosseinpourpia and Mai 2016a, 2016b). Of the proposed mechanisms, Ringman and coworkers concluded that (4) is likely to be the most important (Ringman et al., 2014; Zelinka et al., 2016). Lowered diffusion rates would inhibit fungi by slowing the transport of degrading agents into the wood and also by slowing the transport of degradation products out of the wood to feed the fungus (Goodell et al., 2017).

Inhibiting cell wall diffusion could be an important mechanism by which acetylation imparts decay resistance to wood. However, there are no studies to our knowledge in which diffusion in untreated and acetylated wood has been compared. One study observed that veneers acetylated to 18.1 WPG immersed 48 h in a dilute solution of Fe^{++} absorbed approximately 20 times less Fe than control wood (Hosseinpourpia and Mai, 2016b). However, because no time course data were acquired, we suspect that this study reflects a higher Fe ion binding capacity of unmodified wood compared with acetylated wood, rather than a higher diffusion rate (Hunt et al., 2017).

In this study, experiments were performed to test the hypothesis that the mechanism by which chemical modifications, such as acetylation, impart decay resistance to wood could be the inhibition of diffusion through wood cell walls. We directly observed the moisture-dependence of potassium ion diffusion in different wood cell walls with varying levels of acetylation. .

2. Materials and methods

2.1. Wood

A kiln-dried loblolly pine (*Pinus taeda*) board (2 by 12 in., 5 by 30 cm) was obtained from Shuqualak Lumber in Shuqualak, Mississippi, USA. A single latewood band without compression wood, approximately 3 mm thick and located about 30 cm from the pith, was chosen and used throughout. Specimens prepared for acetylation treatment were typically 3 mm in the radial direction, 5–20 mm in the tangential direction, and 25 mm in the longitudinal direction. Samples were randomly assigned to a level of acetylation.

2.2. Acetylation

The samples used in this study were from the same batch of acetylation treatments used for a previous study, and full treatment details can be found there (Passarini et al., 2017). After immersion in acetic anhydride and reaction for various times at 140 °C, samples were removed, washed in water, and dried. Five individual specimens were used in this study, including the control and acetylation WPGs of 8.1 and 8.2 (pooled to get enough mass for sorption isotherm), 10.9, 13.2, and 20.3, which will be referred to as 8, 11, 13, and 20 WPG, respectively.

2.3. X-ray fluorescence microscopy (XFM)

X-ray fluorescence microscopy (XFM) and an *in situ* RH chamber were used to observe RH-dependent ion diffusion in wood cell walls. XFM is a synchrotron-based technique capable of mapping ions in wood cell walls with high sensitivity and submicron spatial resolution. In previous work on unmodified wood, this technique showed that implanted ions (K^+, Cl^-, Cu^{2+}, Zn^{2+}) in unmodified wood cell walls only diffuse above a threshold RH (Zelinka et al., 2014). Because acetylation is proposed to inhibit diffusion of all chemical species produced by any wood decay organism, any diffusible species would be sufficient to test this hypothesis. The K^+ ion in K_2SO_4 is a good model for decay agents or released degradation products because smaller species such as K^+ generally diffuse faster and K^+ ions tend not to form complexes (Dean, 1992). In addition, K_2SO_4 has a high deliquescence point (96% RH); therefore, the solid salt will not liquefy during the experiments. Finally, the K signal was strong enough to obtain high quality data.

Two-μm-thick sections measuring approximately 2 mm in length and 0.5 mm wide were cut using a diamond knife fit into a Leica EM UC7 ultramicrotome (Wetzlar, Germany). Sections were prepared with both transverse and radial–longitudinal orientations. Sample holders were made from a piece of 0.13-mm-thick Kapton™ (DuPont, Wilmington, Delaware, USA) film with a 1-mm-wide by 5-mm-long slot cut in the center. The wood section ends were secured to the Kapton™ film using small pieces of Kapton™ tape such that the section freely

spanned the 1-mm-wide slot. One sample holder could not hold all the sections. Therefore, one holder was prepared with a transverse section from each of the five treatments, and another holder was prepared with the longitudinal sections. Potassium (K^+) ions were implanted into the sections using a tiny drop of K_2SO_4-saturated aqueous solution that was deposited manually using a sharpened piece of polystyrene foam under a dissecting microscope. The heat from the microscope light caused the water in the drop to evaporate in a couple of seconds, which resulted in an implanted ion front in the wood cell walls.

A sample holder was secured inside of the custom-built RH chamber constructed of an aluminum frame covered by Kapton™ film (Zelinka et al., 2014). The RH was controlled by a HumidiSys™ RH generator (Instruquest, Coconut Creek, Florida, USA) supplied with nitrogen gas. The RH inside the chamber was monitored by a Sensirion SHT1x sensor (Staefa, Switzerland). The RH chamber was placed into beamline 2-ID-E at the Advanced Photon Source at Argonne National Laboratory (Argonne, Illinois, USA) for XFM ion mapping. All XFM mapping was performed under dry condition before or after humidity conditioning steps. The incident X-ray beam energy was 10.2 keV, and the spot size was approximately 0.5 μm diameter. Elemental maps were built in 0.3-μm steps with 5-ms dwell times at each step. All fluorescing elements were mapped, but only relevant elements are discussed. The elemental maps were created using the MAPS software package (Vogt, 2003) in which full spectra were fit to modified Gaussian peaks, the background was iteratively calculated and subtracted, and the results were compared with standard reference materials (RF4-100-S1749, AXO DRESDEN GmbH, Heidenau, Germany).

All longitudinal sections were tested during one run, and the transverse sections were tested during another run. At the beginning of a run, sections were conditioned under dry nitrogen and an initial overview image was collected for each section. From the overview image, a region of interest (ROI) with an ion front in a wood cell was chosen and imaged at high resolution. Then, the RH was changed in a nominal step function to a specified RH. It took about 3 min for the RH chamber to reach the target RH, after which it was held for 10 min at the target RH. The RH was then returned back to dry conditions, and after 10 min of conditioning, each ROI was reimaged. The RH conditioning and imaging steps were repeated using successively higher RH until obvious movement in the implanted ion front was observed. The RH threshold for diffusion was identified by carefully comparing successive images and observing at which RH the ion front changed.

2.4. Sorption isotherms

To relate the RH threshold for K movement observed in XFM to wood EMC, absorption isotherm data were obtained from specimens matching the specimens used to make the sections for XFM. Sorption isotherms were taken using a pseudo-dynamic vapor sorption method using an RH generator and an analytical balance (Zelinka et al., in press). Samples were run in parallel: each RH step was stopped when the change in moisture content (of all samples) as a function of time was less than 0.1 $\mu g\, g^{-1}\, min^{-1}$ for a 24-h period. EMC was then converted to reduced EMC (EMC_R) to allow the moisture content to be expressed on the basis of original wood mass (Akitsu et al., 1993), using the equation.

$$EMC_R = EMC * (1 - WPG)^{-1}.$$

3. Results

XFM Zn, K, and S maps of a 2-μm-thick wood section containing an ion front are shown in Fig. 2. This figure is useful for understanding the outputs from the XFM experiment and how the XFM maps were used in the determination of the RH threshold for ion movement. The map of the native Zn (Fig. 2, Zn) demonstrates the sensitivity of XFM and is also useful to help identify the cell wall features. The horizontal line of increased intensity near the top of the Zn map was identified as the middle lamella because Zn is often more abundant in the middle lamella than the secondary cell walls (Saka and Goring, 1983). The black zero intensity region at the bottom was empty space in the lumen. Between the middle lamella and the lumen was the secondary cell wall. The region of high Zn intensity adjacent to the lumen was probably an upturned flap of tissue. The ion front implanted by the drop of K_2SO_4-saturated solution was identified by the sharp vertical gradient in intensity on the left side of the K and S maps in Fig. 2 K and S, respectively. The matching shapes and locations of the fronts in both the K and S maps confirmed the front was formed by the drop of K_2SO_4-saturated solution. The high intensity finger of K and S in the top left shows where the droplet spread along the S2 layer immediately adjacent to the middle lamella during the drop deposition. The ion front appeared to be much sharper in the K maps because signal to noise ratio was much better for K than for S. Therefore, only K maps were used when determining if ion fronts changed during the RH conditioning steps.

The XFM maps for the experimental run with the longitudinal sections are shown in Fig. 3 with a column for each of the five sections. In the top row of the image (Overview), the largest field of view image of the section is displayed. The signal was either the native Zn in the cell wall or the total scattering, whichever best showed the features of the cell walls. The second row is the same region showing K intensity with a yellow rectangle representing the ROI containing the K front that was monitored during the RH conditioning steps. The remainder of each column shows K maps after exposure to the progressively higher RH conditions indicated in the figure. Some maps are missing because the wood section moved during the RH conditioning step and the obtained XFM map did not encompass the needed ROI. Unfortunately, this mistake was not realized until after the next RH conditioning step; therefore, it was not possible to obtain the missing maps. In each column, two yellow ellipses indicate the RH threshold for K movement. Moving downward, the first ellipse was placed in the map with the highest humidity and no detected ion movement, and the second ellipse was located in the first map with observable ion movement. For the control sections, the ellipses were placed in 60% and 67% RH maps, indicating that the RH threshold for K movement was identified between 60% and 67% RH. The 8, 11, and 13 WPG samples all had the same thresholds for ion mobility, between 77% and 82% RH. For the 20 WPG sample, the ion mobility was detected after exposure to 95% RH; therefore, the threshold was between 92% and 95%. For all sections at and just above the threshold, the amount of K mobility was small and the determination of whether or not ions moved was subjective. However, as the RH increased, the amount of K movement increased and ion movement became very obvious. One strategy used to help determine whether or not the subtle ion movement was real was to look at the maps after conditioning at higher RH to check that increasing ion movements stemmed from the identified areas of initial K movements.

Fig. 4 shows the XFM maps for the experimental run with transverse sections. The 13 WPG section did not have an adequate K front; therefore, experiments could not be performed on that section. As in Fig. 3, the top two rows contain the overview maps and the yellow rectangles in the K maps indicate the ROI presented in successive K maps down each column. In the control, the first section that displayed movement was after the 75% RH conditioning, especially compared with the 60% RH K map. It was inconclusive whether movement also occurred after the 65% and 69% RH steps. Therefore the 60%–75% RH range was chosen for the transverse control RH threshold. In the remaining sections, threshold RH ranges of 75–87%, 65–79%, and 87–95% were identified for 8, 11, and 20 WPG, respectively. In some of the K maps in the 8 and 20 WPG sections, there is an artifact marked with a red x. The artifact is a transient bright region visible in the K map, which was even stronger in the Ca and P maps (not shown). We suspect this artifact was a contaminant of some type that moved with the wall of the RH chamber. We excluded from consideration maps with K fronts that were affected by the contaminant, such as the 79% RH

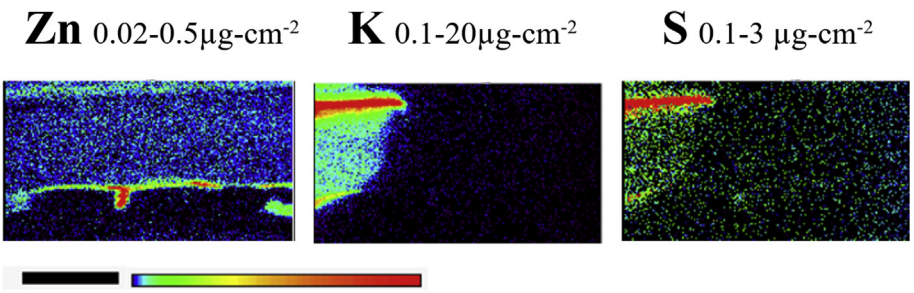

Fig. 2. Example X-ray fluorescence microscopy (XFM) Zn (left), K (center), and S (right) maps of an unacetylated longitudinal section with implanted ions. The Zn was naturally occurring and useful for identifying the wood structure. The K and S maps clearly show the K and S implanted with the K_2SO_4-saturated aqueous solution. Color intensities are displayed in a log scale across the ranges indicated for each map. The scale bar is 20 µm. (For interpretation of the references to color in this figure legend, the reader is referred to the Web version of this article.)

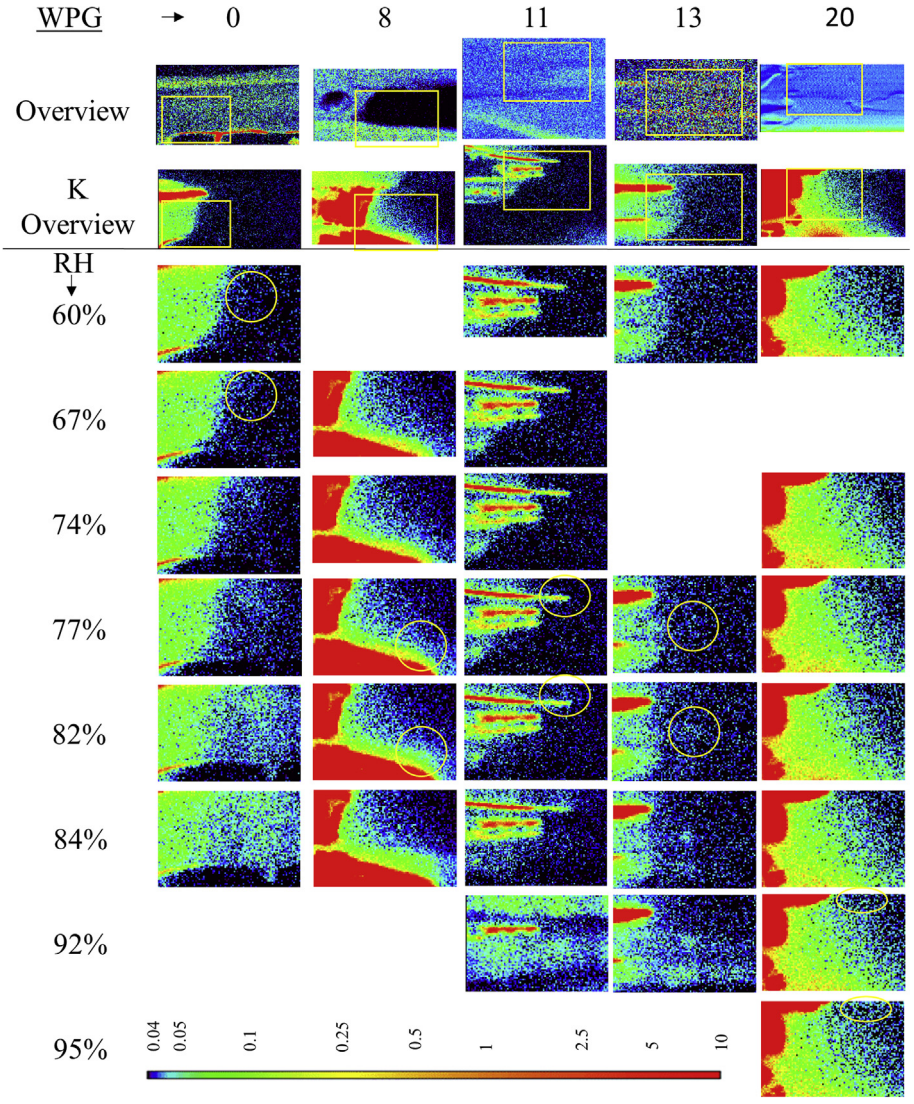

Fig. 3.. X-ray fluorescence microscopy (XFM) maps of the experimental run with longitudinal sections. The acetylation weight percentage gain (WPG) is shown at the top for each column. The "Overview" row displays maps of either Zn or total scattering, whichever best showed the cellular structure. The "K Overview" row is the K map of the same region. The yellow rectangles in the overview rows outline the 28 by 19 µm regions shown below after conditioning at the indicated relative humidity (RH). The yellow ellipses indicate the RH and locations where movement in the K front was first observed. The color intensities are displayed in a log scale from 0.04 to 10 µg-cm^{-2}.

image of the 8 WPG.

The identified RH thresholds are summarized in Fig. 5a. Following the pairs of ellipses in Figs. 3 and 4, the vertical bars extend from the highest RH without movement to the lowest RH with movement. For the control samples, the K^+ RH thresholds agreed with previous work using unmodified loblolly pine latewood sections in which K^+ was implanted with a KCl aqueous solution and the threshold was observed to be between 60% and 65% RH in both transverse and longitudinal orientations (Zelinka et al., 2014). The RH threshold for K^+ movement increased with acetylation, and thresholds for transverse and longitudinal sections all overlap for a given WPG. The 8, 11, and 13 WPG sections all have RH thresholds intermediate to the control and the 20 WPG section. The trend of increasing RH thresholds with increasing WPG in Fig. 5a correlates with the dependency of decay resistance on acetylation WPG. As previously stated, acetylation around 10 WPG is only mildly inhibitory to decay, whereas acetylation at greater than 16 WPG is effective at inhibiting decay in lab testing, and 20 WPG is even more decay resistant in field tests. This suggests that the onset of K diffusion may indicate a relative degree of decay resistance.

To better understand the role of moisture content on K^+ diffusion, the RH thresholds were converted to EMC values using the absorption isotherms. The EMC thresholds (Fig. 5b) decreased with increasing WPG. However, for chemically modified wood, the EMC may not be the most appropriate measure of moisture content because even if the modified wood holds the same amount of water as unmodified wood, the EMC of the modified wood would be lower because the oven-dry

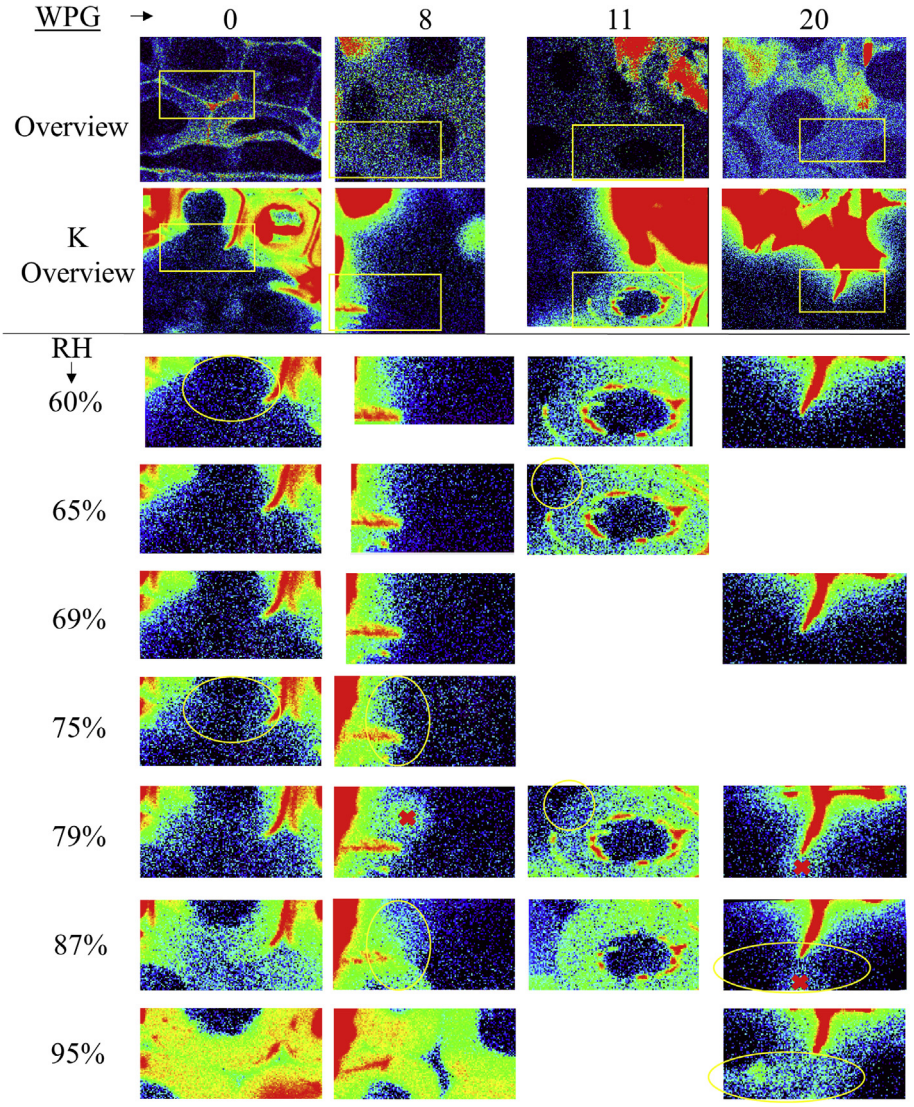

Fig. 4. X-ray fluorescence microscopy (XFM) maps of the experimental run with transverse sections. The acetylation weight percentage gain (WPG) is shown at the top for each column. The "Overview" row displays maps of either Zn or total scattering, whichever best showed the cellular structure. The "K Overview" row is the K map of the same region. The yellow rectangles in the overview row outline the 40 by 20 μm regions shown below after conditioning at the indicated relative humidity (RH). The yellow ellipses indicate the RH and locations where movement in the K front was first observed. The red x denotes an identified artifact. The color intensities are displayed in a log scale from 0.04 to 10 μg-cm^{-2}.

mass of the modified wood includes the added mass from the modification (Hill, 2008). The EMC_R is therefore considered a better metric for chemically modified wood to compare the relative amounts of absorbed moisture (Thybring, 2013). The calculated EMC_R thresholds for first ion movement are plotted in Fig. 5c. With the limited amount of data available, there does not appear to be a clear trend of threshold EMC_R with acetylation WPG, although a slight decrease of threshold EMC_R at high WPG may be evident. If decreasing the bulk wood moisture content was the controlling factor for cell wall diffusion in acetylated wood, then the threshold for diffusion should occur at the same EMC_R independent of acetylation WPG. A trend of the EMC_R threshold with acetylation WPG would mean that another factor is probably influencing diffusion. These data, however, are not strong enough to make a conclusion either way.

Qualitative observations about the effect of RH on the rate of ion movement can also be made from the K maps that were obtained after conditioning at RH above the thresholds in Figs. 3 and 4. It is evident that K mobility increased dramatically with RH after it was above the movement threshold for both control and acetylated wood. This is clearly seen in the control longitudinal section in the first column of Fig. 3. The amount of movement that occurred during the 74% RH step, which can be observed by visually comparing the K front in the 67% RH map to the front in the 74% RH map, is much smaller than the amount of K movement that occurred during the 82% RH step. Similarly, in the 8 WPG transverse section in Fig. 4, the combined amount of K movement that occurred during 69%, 75%, and 79% RH steps was much smaller than the amount of movement observed during the 87% RH step. Compared with the control sections, large amounts of diffusion were not observed in 20 WPG sections even up to 95% RH. These observations suggest that even if acetylation did not completely stop diffusion under the high moisture conditions conducive to decay, acetylation may still have slowed diffusion through cell walls enough to inhibit decay, especially in the 20 WPG specimen which is expected to be very decay resistant.

4. Discussion

The objective of this study was to experimentally determine whether or not diffusion was inhibited in acetylated wood. These XFM experiments conclusively demonstrated that the diffusion of implanted K^+ ions were inhibited by acetylation, especially as evidenced by the increased RH threshold with acetylation WPG in Fig. 5a. This increased RH threshold with acetylation WPG was found to be similar to the increase in decay resistance with WPG in acetylated wood, which supports the proposed mechanism that acetylation inhibits decay by inhibiting diffusion through the wood cell walls. However, these results do not confirm it as the most important mechanism. Other mechanisms for decay resistance were not addressed by these data. It is also possible

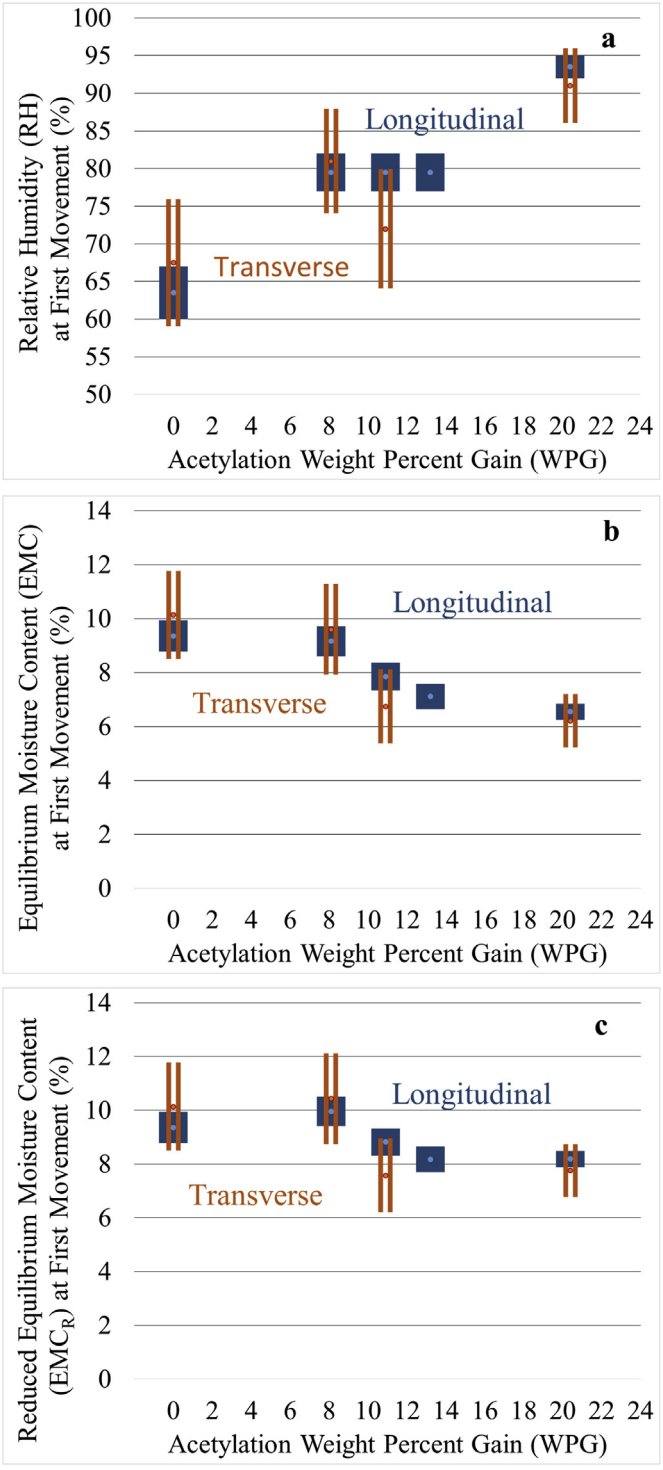

Fig. 5. Threshold vs. WPG. Observed (a) relative humidity (RH), (b) equilibrium moisture content (EMC), and (c) reduced equilibrium moisture content (EMC_R) thresholds for K movement as a function of acetylation. The plotted thresholds span from the highest RH without observable K movement to the lowest RH where movement was observed, following the ellipses in Fig. 3 and 4.

that the observed K^+ transport behaved differently than the diffusion of the chemicals relevant to decay. Although some agents important to brown rot, such as Fe^{3+}, are cationic similar to our K^+ probe and some are neutral (H_2O_2, dimethoxyhydroquinone-derived radicals, released sugars) (Hammel et al., 2002; Arantes and Goodell, 2014), the mechanisms subsequently discussed for the restriction of diffusion with acetylation are relevant to both ionic and nonionic diffusible species. It might also be that the thresholds for K^+ transport only happen to correlate with decay resistance and another mechanism controls decay resistance.

These results provide strong motivation for additional work studying diffusion through chemically modified wood cell walls and its potential implications for decay resistance. Particularly, the way chemicals transport through wood cell walls needs to be better understood. A recently proposed model for chemical transport through wood cell walls is a useful tool to help identify the potential mechanisms by which chemical modifications such as acetylation inhibit diffusion. In the model, it was proposed that transport occurs via pathways of a percolated, interconnecting network formed by regions of hemicelluloses and amorphous cellulose that have passed through their moisture-induced glass transition (Zelinka et al., 2008; Jakes et al., 2013; Plaza et al., 2016). This model is supported by the observation that the RH threshold for ion transport observed with these XFM experiments for unmodified wood falls within the 60–80% RH range in which hemicelluloses pass through their moisture-induced glass transition. Zelinka and coworkers used this model to help identify how chemical modifications such as acetylation may be inhibiting cell wall diffusion (Zelinka et al., 2016). They proposed that a modification may be preventing the hemicelluloses and amorphous cellulose from passing through their moisture-induced glass transition or the modification may be preventing the softened regions from forming an interconnected pathway. Although the current experiments do not distinguish between these two proposed mechanisms, they do provide the important information that indeed diffusion is inhibited in acetylated wood cell walls. Therefore, it is worthwhile to put more effort into identifying if either of the proposed mechanisms are relevant. If the mechanism is identified, it would enable the development and improvement of non-toxic wood treatments for decay resistance. The next step to identifying the mechanism would be to perform experiments, such as mechanical spectroscopy, to determine whether or not acetylation affects the moisture-induced glass transition of hemicelluloses and amorphous cellulose.

If the hemicelluloses are primarily responsible for diffusion within the cell wall, the best measure of acetylation with respect to inhibiting decay may not be the WPG. Generally, the rate of hydroxyl groups acetylated follows the order lignin > hemicelluloses > cellulose, which is proposed to be mostly a function of accessibility to the acetic anhydride reagent (Rowell, 1982; Hill, 2006; Sadeghifar et al., 2014). Consequentially, at lower WPG, the extent of lignin modification is much higher than the hemicelluloses and cellulose. For example, Rowell and coworkers estimated that at 8 WPG, about 80% of accessible hydroxyl groups on lignin were modified, whereas only 12% were modified in the holocellulose (Rowell et al., 1994). At 18% WPG, they estimated that nearly all lignin hydroxyl groups were modified and only 20% of the holocellulose hydroxyl groups were modified. Even though the percentage of holocellulose hydroxyl group modification was based on the total number of hydroxyl groups present, which included inaccessible hydroxyl groups inside of the semicrystalline cellulose fibrils, the results suggest that substantial acetylation of hemicelluloses did not occur until the higher WPGs. This might explain the potential decrease of the EMC_R threshold with higher WPG in Fig. 5c because acetylation occurring at the higher WPG was in the hemicelluloses and more effective at inhibiting diffusion. If hemicelluloses are responsible for diffusion and decay, then the more effective parameter may be the degree of modification of hemicelluloses. Furthermore, reaction conditions that favor modification of hemicelluloses relative to lignin might result in more diffusion inhibition, and possible better decay resistance, for the same extent of reaction.

It is also possible that the glass transition of hemicelluloses is not important to diffusion through wood cell walls or the mechanism of decay. Because acetylated wood has a lower moisture content than unmodified wood at a given RH, the diffusion of ions might be inhibited simply from having less solvation water (Thygesen et al., 2010; Popescu

et al., 2014). The water solvates both the diffusing species and the polymers; this is sometimes described in terms of a lack of free volume inside the cell wall (Papadopoulos and Hill, 2002; Boonstra and Tjeerdsma, 2006). Thybring, by analyzing the data of many researchers, found that different types of chemical modifications (bulking, grafting, and cross-linking) all exhibited a threshold for decay resistance when EMC of the modified wood was decreased by approximately 40% compared with unmodified wood (Thybring, 2013). This further supports the idea that simply limiting moisture and the accompanying free volume inside the cell wall may be the key to inhibiting diffusion and decay. However, with these limited data (Fig. 5c), it was not possible to conclude whether or not the observed thresholds for K^+ transport were being controlled only by the amount of absorbed moisture.

5. Conclusions

The experiments show that chemically modifying wood by acetylation increased the RH threshold for diffusion within wood cell walls. In addition, the rate of K^+ movement at a given RH level appeared to decrease as the level of acetylation increased. Both these results are consistent with the proposed mechanism that acetylation and other chemical modifications inhibit decay by restricting the transport of fungal degradation agents and the resulting degradation products through the wood cell wall.

Acknowledgements

This research used resources of the Advanced Photon Source, a U.S. Department of Energy (DOE) Office of Science User Facility operated for the DOE Office of Science by Argonne National Laboratory under Contract No. DE-AC02-06CH11357. The authors thank the machine shop at the Forest Products Laboratory for construction of the *in situ* relative humidity chamber, and to the reviewers and editor for helpful comments.

References

Akitsu, H., Norimoto, M., Morooka, T., Rowell, R.M., 1993. Effect of humidity on vibrational properties of chemically modified wood. Wood Fiber Sci. 25, 250–260. https://wfs.swst.org/index.php/wfs/article/view/1546, Accessed date: 24 May 2018.

Alfredsen, G., Ringman, R., Pilgård, A., Fossdal, C., 2015. New insight regarding mode of action of brown rot decay of modified wood based on DNA and gene expression studies: a review. Int. Wood Prod. J. 6, 5–7. https://doi.org/10.1179/2042645314Y.0000000085.

Arantes, V., Goodell, B., 2014. Current understanding of brown-rot fungal biodegradation mechanisms: a review. In: Schultz, T. (Ed.), Deterioration and Protection of Sustainable Biomaterials. ACS, Washington, DC ACS Symposium Series, #1158, 3–21. https://doi.org/10.1021/bk-2014-1158.ch001.

Bergman, R., Puettmann, M., Taylor, A., Skog, K.E., 2014. The carbon impacts of wood products. For. Prod. J. 64, 220–231. https://doi.org/10.13073/FPJ-D-14-00047.

Boonstra, M., Van Acker, J., Kegel, E., Stevens, M., 2007. Optimisation of a two-stage heat treatment process: durability aspects. Wood Sci. Technol. 41, 31–57. https://doi.org/10.1007/s00226-006-0087-4.

Boonstra, M.J., Tjeerdsma, B., 2006. Chemical analysis of heat treated softwoods. Holz als Roh- Werkst. 64, 204–211. https://doi.org/10.1007/s00107-005-0078-4.

Cohen, R., Jensen, K.A., Houtman, C.J., Hammel, K.E., 2002. Significant levels of extracellular reactive oxygen species produced by brown rot basidiomycetes on cellulose. FEBS (Fed. Eur. Biochem. Soc.) Lett. 531, 483–488. https://doi.org/10.1016/S0014-5793(02)03589-5.

Curling, S.F., Clausen, C.A., Winandy, J.E., 2002. Relationships between mechanical properties, weight loss, and chemical composition of wood during incipient brown-rot decay. For. Prod. J. 52, 34–39.

Dean, J.A., 1992. The group I elements: Li, Na, K, Rb, Cs. In: Lange's Handbook of Chemistry. McGraw-Hill, New York, pp. 189–205.

Engelund, E.T., Thygesen, L.G., Svensson, S., Hill, C.A., 2013. A critical discussion of the physics of wood–water interactions. Wood Sci. Technol. 47, 141–161.

Goodell, B., Zhu, Y., Kim, S., Kafle, K., Eastwood, D., Daniel, G., Jellison, J., Yoshida, M., Groom, L., Pingali, S.V, 2017. Modification of the nanostructure of lignocellulose cell walls via a non-enzymatic lignocellulose deconstruction system in brown rot wood-decay fungi. Biotechnol. Biofuels 10 (179). https://doi.org/10.1186/s13068-017-0865-2.

Hammel, K., Kapich, A., Jensen, K., Ryan, Z., 2002. Reactive oxygen species as agents of wood decay by fungi. Enzym. Microb. Technol. 30, 445–453. https://doi.org/10.1016/S0141-0229(02)00011-X.

Harvey, P.J., Schoemaker, H.E., Palmer, J.M., 1986. Veratryl alcohol as a mediator and the role of radical cations in lignin biodegradation by Phanerochaete chrysosporium. FEBS (Fed. Eur. Biochem. Soc.) Lett. 195, 242–246. https://doi.org/10.1016/0014-5793(86)80168-5.

Hill, C.A., 2011. Wood modification: an update. J. Bioresour 6, 918–919.

Hill, C.A.S., 2006. Wood Modification: Chemical, Thermal, and Other Processes. John Wiley and Sons, New York.

Hill, C.A.S., 2008. The reduction in the fibre saturation point of wood due to chemical modification using anhydride reagents: a reappraisal. Holzforschung 62, 423–428. https://doi.org/10.1515/HF.2008.078.

Hill, C.A.S., 2009. Why does acetylation protect wood from microbiological attack? Wood Mater. Sci. Eng. 4, 37–45. https://doi.org/10.1080/17480270903249409.

Hill, C.A.S., Forster, S.C., Farahani, M.R.M., Hale, M.D.C., Ormondroyd, G.A., Williams, G.R., 2005. An investigation of cell wall micropore blocking as a possible mechanism for the decay resistance of anhydride modified wood. Int. Biodeterior. Biodegrad. 55, 69–76. https://dx.doi.org/10.1016/j.ibiod.2004.07.003.

Hill, C.A.S., Graham, O.A., 2004. Dimensional changes in Corsican pine (Pinus nigra Arnold) modified with acetic anhydride measured using a helium pycnometer. Holzforschung 58 (544). https://doi.org/10.1515/hf.2004.082.

Hosseinpourpia, R., Mai, C., 2016a. Mode of action of brown rot decay resistance in phenol-formaldehyde-modified wood: resistance to Fenton's reagent. Holzforschung 70, 253–259. https://doi.org/10.1515/hf-2015-0045.

Hosseinpourpia, R., Mai, C., 2016b. Mode of action of brown rot decay resistance of acetylated wood: resistance to Fenton's reagent. Wood Sci. Technol. 50, 413–426. https://doi.org/10.1007/s00226-015-0790-0.

Hunt, C.G., Lacher, S., Hirth, K., Lorenz, L., Hammel, K.E., Houtman, C.J., Thybring, E.E., Zelinka, S.L., 2017. Exploring the hypothesis that limiting diffusion of fungal oxidants underlies decay resistance in acetylated wood. In: COST Action FP1407 "Wood modification research and applications", Kuchl, Austria, Salzburg University of Applied Sciences, . https://fh-salzburg.ac.at/fileadmin/fh/forschung/holz-biogene-tech/documents/Publikationen/2017_COST1407Conf_-_dig._proceedings_final.pdf#page=38, Accessed date: 24 May 2018.

Ibach, R.E., Rowell, R.M., 2000. Improvements in decay resistance based on moisture exclusion. Molecular crystals and liquid crystals science and technology. Section a. Mol. Cryst. Liq. Cryst. 353, 23–33. https://doi.org/10.1080/10587250008025645.

Jakes, J.E., Arzola, X., Bergman, R., Ciesielski, P., Hunt, C.G., Rahbar, N., Tshabalala, M., Wiedenhoeft, A.C., Zelinka, S.L., 2016. Not just lumber - using wood in the sustainable future of materials, chemicals, and fuels. JOM (J. Occup. Med.) 68, 2395–2404. https://doi.org/10.1007/s11837-016-2026-7.

Jakes, J.E., Plaza, N., Stone, D.S., Hunt, C.G., Glass, S.V., Zelinka, S.L., 2013. Mechanism of transport through wood cell wall polymers. J. For. Prod. Ind. 2, 10–13. https://www.fpl.fs.fed.us/documnts/pdf2013/fpl_2013_jakes002.pdf, Accessed date: 24 May 2018.

Kerem, Z., Bao, W., Hammel, K.E., 1998. Rapid polyether cleavage via extracellular one-electron oxidation by a brown-rot basidiomycete. Proc. Natl. Acad. Sci. U.S.A. 95, 10373–10377.

Larsson Brelid, P., Simonson, R., Bergman, Ö., Nilsson, T., 2000. Resistance of acetylated wood to biological degradation. Holz als Roh- Werkst. 58, 331–337. https://doi.org/10.1007/s001070050439.

Lebow, S., 2004. Alternatives to chromated copper arsenate for residential construction. FPL-RP-618. U.S. Department of Agriculture. In: Forest Service, Forest Products Laboratory. Madison,, WI, pp. 9. https://doi.org/10.2737/FPL-RP-618.

Mantanis, G.I., 2017. Chemical modification of wood by acetylation or furfurylation: a review of the present scaled-up technologies. J. Bioresour 12, 4478–4489.

Martinez, A.T., Speranza, M., Ruiz-Duenas, F.J., Ferreira, P., Camarero, S., Guillen, F., Martinez, M.J., Gutierrez, A., del Rio, J.C., 2005. Biodegradation of lignocellulosics: microbial chemical, and enzymatic aspects of the fungal attack of lignin. Int. Microbiol. 8, 195–204.

Papadopoulos, A.N., Hill, C.A.S., 2002. The biological effectiveness of wood modified with linear chain carboxylic acid anhydrides against Coniophora puteana. Holz als Roh- Werkst. 60, 329–332. https://doi.org/10.1007/s00107-002-0327-8.

Passarini, L., Zelinka, S.L., Glass, S.V., Hunt, C.G., 2017. Effect of weight percent gain and experimental method on fiber saturation point of acetylated wood determined by differential scanning calorimetry. Wood Sci. Technol. 51, 1291–1305. https://doi.org/10.1007/s00226-017-0963-0.

Plaza, N.Z., Pingali, S.V., Qian, S., Heller, W.T., Jakes, J.E., 2016. Informing the improvement of forest products durability using small angle neutron scattering. Cellulose 23, 1593–1607. https://doi.org/10.1007/s10570-016-0933-y.

Popescu, C.-M., Hill, C.A., Curling, S., Ormondroyd, G., Xie, Y., 2014. The water vapour sorption behaviour of acetylated birch wood: how acetylation affects the sorption isotherm and accessible hydroxyl content. J. Mater. Sci. 49, 2362–2371. https://doi.org/10.1007/s10853-013-7937-x.

Popp, J.L., Kalyanaraman, B., Kirk, T.K., 1990. Lignin peroxidase oxidation of Mn2+ in the presence of veratryl alcohol, malonic or oxalic acid, and oxygen. Biochemistry 29, 10475–10480. https://doi.org/10.1021/bi00498a008.

Ringman, R., Pilgård, A., Brischke, C., Richter, K., 2014. Mode of action of brown rot decay resistance in modified wood: a review. Holzforschung 68, 239–246. https://doi.org/10.1515/hf-2013-0057.

Rowell, R., 1982. Distribution of acetyl groups in southern pine reacted with acetic anhydride. Wood Sci. 15, 172–182.

Rowell, R., 2005. Ch 14: chemical modification of wood. In: Rowell, R. (Ed.), Handbook of Wood Chemistry and Wood Composites. Taylor & Francis, Boca Raton, pp. 381–420.

Rowell, R., 2015. Correlation between equilibrium moisture content and resistance to decay by brown-rot fungi on acetylated wood. In: Eighth European Conference on

Wood Modification, Helsinki, Finland.
Rowell, R., Simonson, R., Hess, S., Plackett, D., Cronshaw, D., Dunningham, E., 1994. Acetyl distribution in acetylated whole wood and reactivity of isolated wood cell-wall components to acetic anhydride. Wood Fiber Sci. 26, 11–18. https://wfs.swst.org/index.php/wfs/article/view/541, Accessed date: 24 May 2018.
Rowell, R.M., Ibach, R.E., McSweeny, J., Nilsson, T., 2009. Understanding decay resistance, dimensional stability and strength changes in heat-treated and acetylated wood. Wood Mater. Sci. Eng. 4, 14–22. https://doi.org/10.1080/17480270903261339.
Sadeghifar, H., Dickerson, J.P., Argyropoulos, D.S., 2014. Quantitative 31P NMR analysis of solid wood offers an insight into the acetylation of its components. Carbohydr. Polym. 113, 552–560. https://doi.org/10.1016/j.carbpol.2014.07.046.
Saka, S., Goring, D.A., 1983. The distribution of inorganic constituents in black spruce wood as determined by TEM-EDXA. J. Jpn. Wood Res. Soc. 29, 648–656.
Sandberg, D., Kutnar, A., Mantanis, G., 2017. Wood modification technologies-a review. iFor. Biogeosci. For. 10 (895). https://doi.org/10.3832/ifor2380-010.
Stamm, A.J., Baechler, R.H., 1960. Decay resistance and dimensional stability of five modified woods. For. Prod. J. 10, 22–26.
Stamm, A.J., Tarkow, H., 1947. Dimensional stabilisation of wood. J. Colloid Sci. 51, 493–505.
Suzuki, M.R., Hunt, C.G., Houtman, C.J., Dalebroux, Z.D., Hammel, K.E., 2006. Fungal hydroquinones contribute to brown rot of wood. Environ. Microbiol. 8, 2214–2223. https://doi.org/10.1111/j.1462-2920.2006.01160.x.
Tanaka, H., Itakura, S., Enoki, A., 1999. Hydroxyl radical generation by an extracellular low-molecular-weight substance and phenol oxidase activity during wood degradation by the white-rot basidiomycete *Trametes versicolor*. J. Biotechnol. 75, 57–70. https://doi.org/10.1016/S0168-1656(99)00138-8.
ten Have, R., Teunissen, P.J., 2001. Oxidative mechanisms involved in lignin degradation by white-rot fungi. Chem. Rev. 101, 3397–3414. https://doi.org/10.1021/cr000115l.
Thybring, E.E., 2013. The decay resistance of modified wood influenced by moisture exclusion and swelling reduction. Int. Biodeterior. Biodegrad. 82, 87–95. https://doi.org/10.1016/j.ibiod.2013.02.004.
Thybring, E.E., 2017. Water relations in untreated and modified wood under brown-rot and white-rot decay. Int. Biodeterior. Biodegrad. 118, 134–142. https://doi.org/10.1016/j.ibiod.2017.01.034.
Thygesen, L.G., Tang Engelund, E., Hoffmeyer, P., 2010. Water sorption in wood and modified wood at high values of relative humidity. Part I: results for untreated, acetylated, and furfurylated Norway spruce. Holzforschung 64, 315–323. https://doi.org/10.1515/hf.2010.044.
Vogt, S., 2003. MAPS: a set of software tools for analysis and visualization of 3D X-ray fluorescence data sets. J. Phys. IV 20030160. https://doi.org/10.1051/jp4.
Xie, Y., Xiao, Z., Mai, C., 2015. Degradation of chemically modified Scots pine (Pinus sylvestris L.) with Fenton reagent. Holzforschung 69, 153. https://doi.org/10.1515/hf-2014-0067.
Zelinka, S., Ringman, R., Pilgård, A., Thybring, E., Jakes, J., Richter, K., 2016. The role of chemical transport in the brown-rot decay resistance of modified wood. Int. Wood Prod. J. 7, 66–70. https://doi.org/10.1080/20426445.2016.1161867.
Zelinka, S.L., Bourne, K.J., Glass, S.V., Boardman, C.R., Lorenz, L. and Thybring, E.E. (in press). Apparatus for gravimetric measurement of moisture sorption isotherms for 1-100 g samples in parallel. Wood Fiber Sci. 50.
Zelinka, S.L., Glass, S.V., Stone, D.S., 2008. A percolation model for electrical conduction in wood with implications for wood-water relations. Wood Fiber Sci. 40, 544–552. https://wfs.swst.org/index.php/wfs/article/view/270, Accessed date: 24 May 2018.
Zelinka, S.L., Gleber, S.-C., Vogt, S., Rodriguez Lopez, G.M., Jakes, J.E., 2014. Threshold for ion movements in wood cell walls below fiber saturation observed by X-ray fluorescence microscopy (XFM). Holzforschung 69, 441–448. https://doi.org/10.1515/hf-2014-0138.